Supplemental Information for

Hilltop curvature as a proxy for erosion rate: Wavelets enable rapid computation and reveal systematic underestimation

William T. Struble[1,2], Joshua J. Roering[2]

[1]Department of Geosciences, University of Arizona, Tucson, Arizona, USA

[2]Department of Earth Sciences, University of Oregon, Eugene, Oregon, USA

Contents of this file:

Figures S1-S10

The supplemental figures in this file include: 1) C_{HT} and erosion rate estimations for all mapped hilltops at Hadsall Creek, North Fork Smith River, and Bear Creek (companion figure to Fig. 5); 2) Visualization of synthetic hillslopes with white noise added (companion figure to Fig. 7, 8); 3) Hilltop curvature measurements for σ=0.5%L_H case for range of E*; 4) Standard deviation of C_{HT} for σ=0.5%L_H case for range of E*; 5-7) Ratio of C_{HT}, C_{HT}, and standard deviation of C_{HT} for σ=0.1%L_H case for range of E*; 8-10) Ratio of C_{HT}, C_{HT}, and standard deviation of C_{HT} for σ=5%L_H case for range of E*.

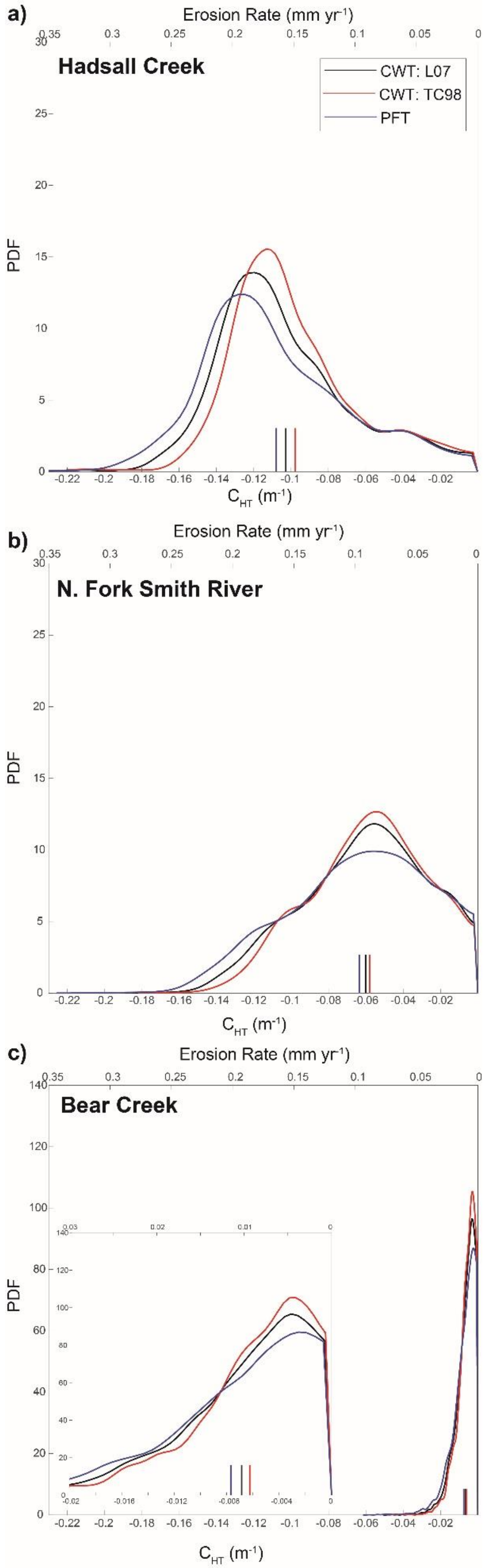

Figure S1: Probability density functions of $C_{HT\text{-}P}$ and $C_{HT\text{-}W}$ and erosion rate calculated using Equation 1 for all mapped hilltops at each OCR field site. See Figure 5 for representative hilltop PDFs for each catchment. Note agreement between each C_{HT} measurement technique. Further, note dramatic variability in C_{HT} between all site (all panels use same x-axis; inset in panel C more clearly displays distribution of C_{HT} at Bear Creek). Small vertical lines at bottom of each panel represent the mean of the plotted distribution (Table 2). Note that positive C_{HT} values are not permitted in the output PDF.

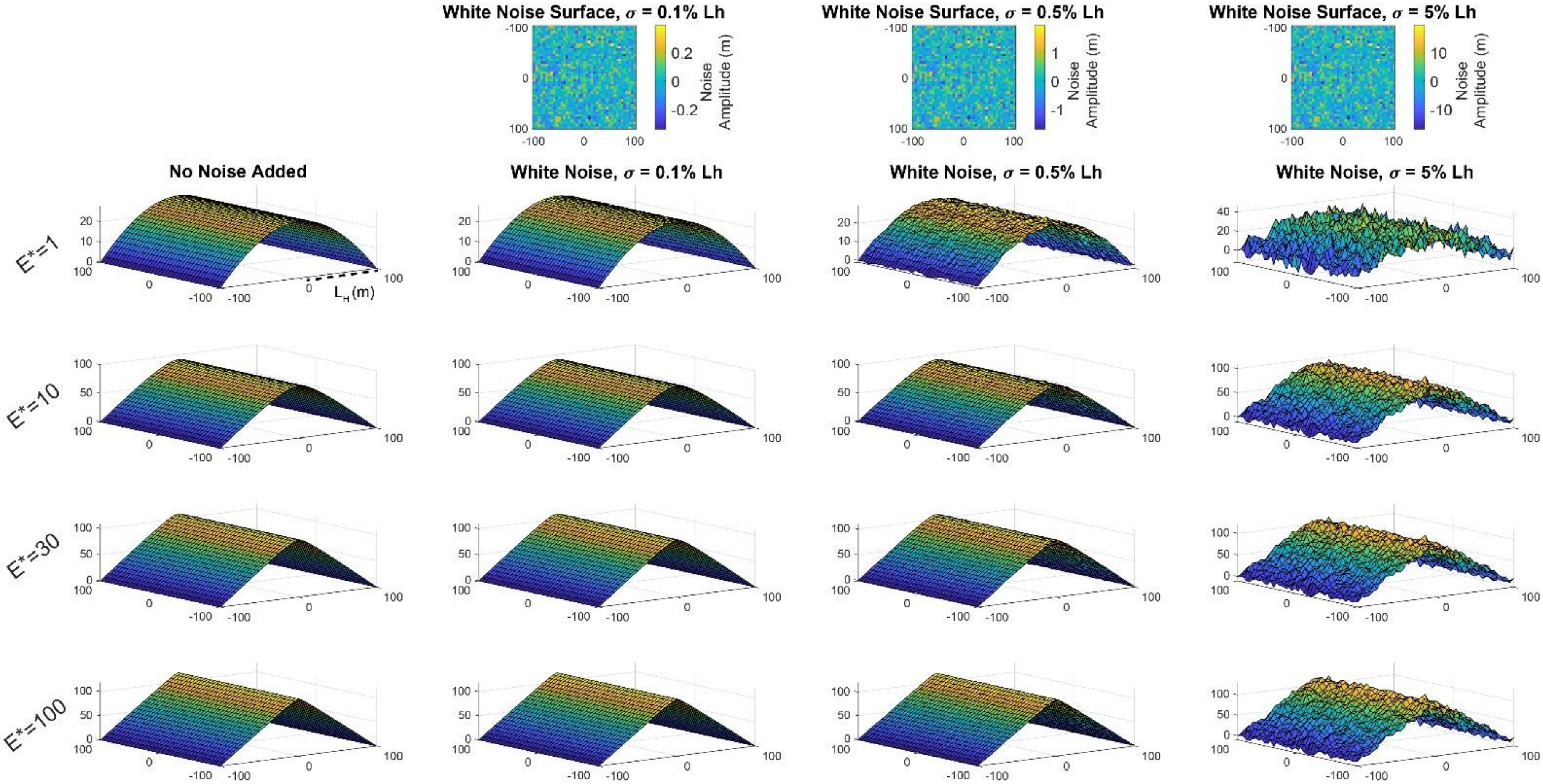

Figure S2: Synthetic hillslopes constructed using Equation 9. Upper row shows white noise surfaces that are added to the original hillslope form (left column); yellow colors correspond with positive deviations from the hillslope (convex noise) and blue with negative deviations (concave noise). Each row of hillslopes corresponds with various dimensionless erosion rates, from E*=1-100. Note the increased prominence of planar hillslopes as E* increases. Noise does not vary with E*; thus the magnitude of noise relative to hillslope relief is more visually apparent at lower E* (See σ=5% L_H column for clear example). Note that noise exhibits little randomness at long-wavelengths, which is apparent in the pink and red noise hillslopes in Figures 7 and 8.

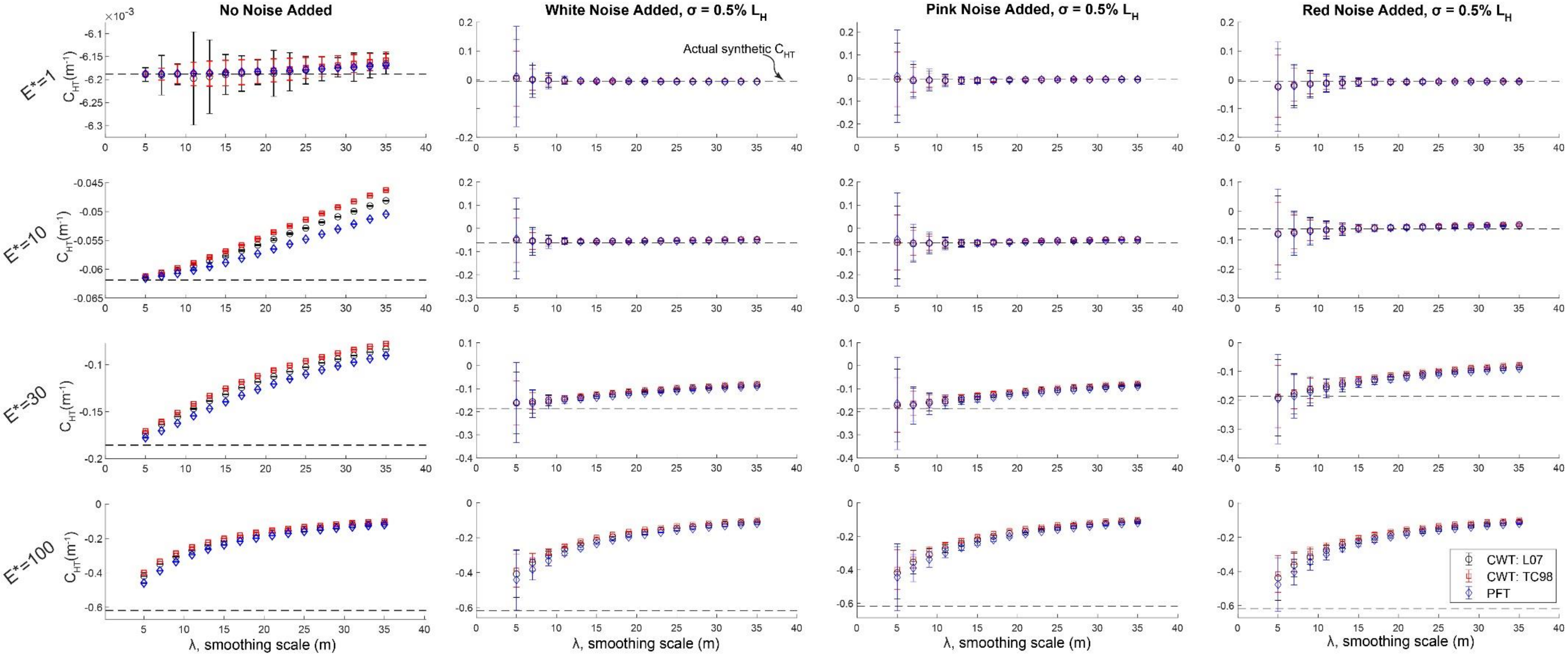

Figure S3: Hilltop curvature when noise amplitude σ=0.5% L_H. E* increases from E*=1 in top row to E*=100 in bottom row. Left column corresponds to synthetic hillslope is no added noise, while columns 2-4 correspond with hillslopes where white, pink, and red noise have been added, respectively. Error bars are 1σ standard deviation on the hilltop. Dashed black line is model-specified C_{HT} for the synthetic hillslope. For clarity of deviation between measured and known C_{HT}, see the ratio of the two values in Figure 9.

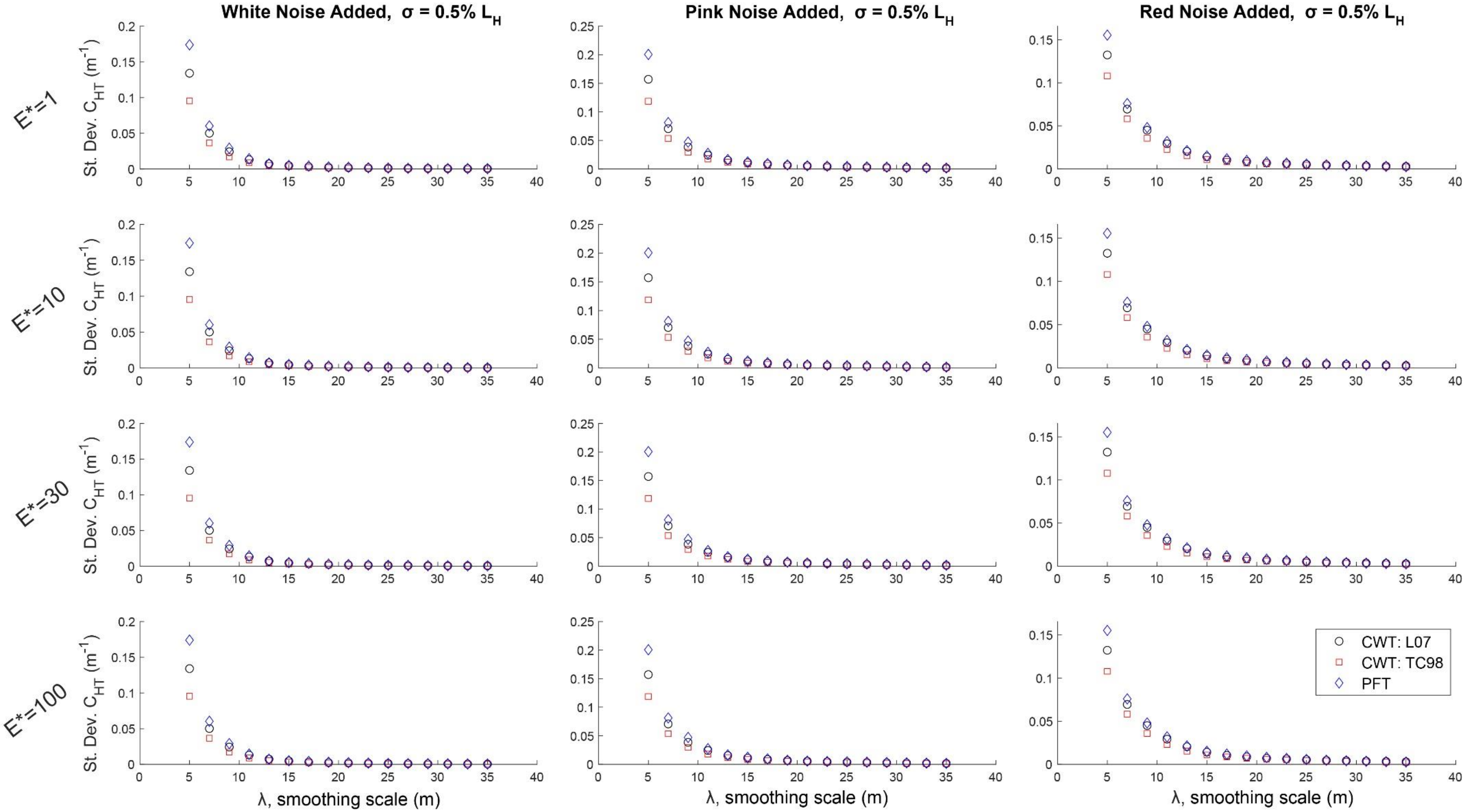

Figure S4: Standard deviation of C_{HT} for noise amplitude σ=0.5%L_H. These values correspond to the error bars in Figure S3. Note that surface noise does not vary as a function of E*. Therefore, given the distributive property of convolutions (see main text for details), the standard deviation does not vary with E*. Note that the standard deviation is high at small smoothing scales when the signal to noise ratio is high. As topography is smoothed, the uncertainty in C_{HT} along the hilltop decreases.

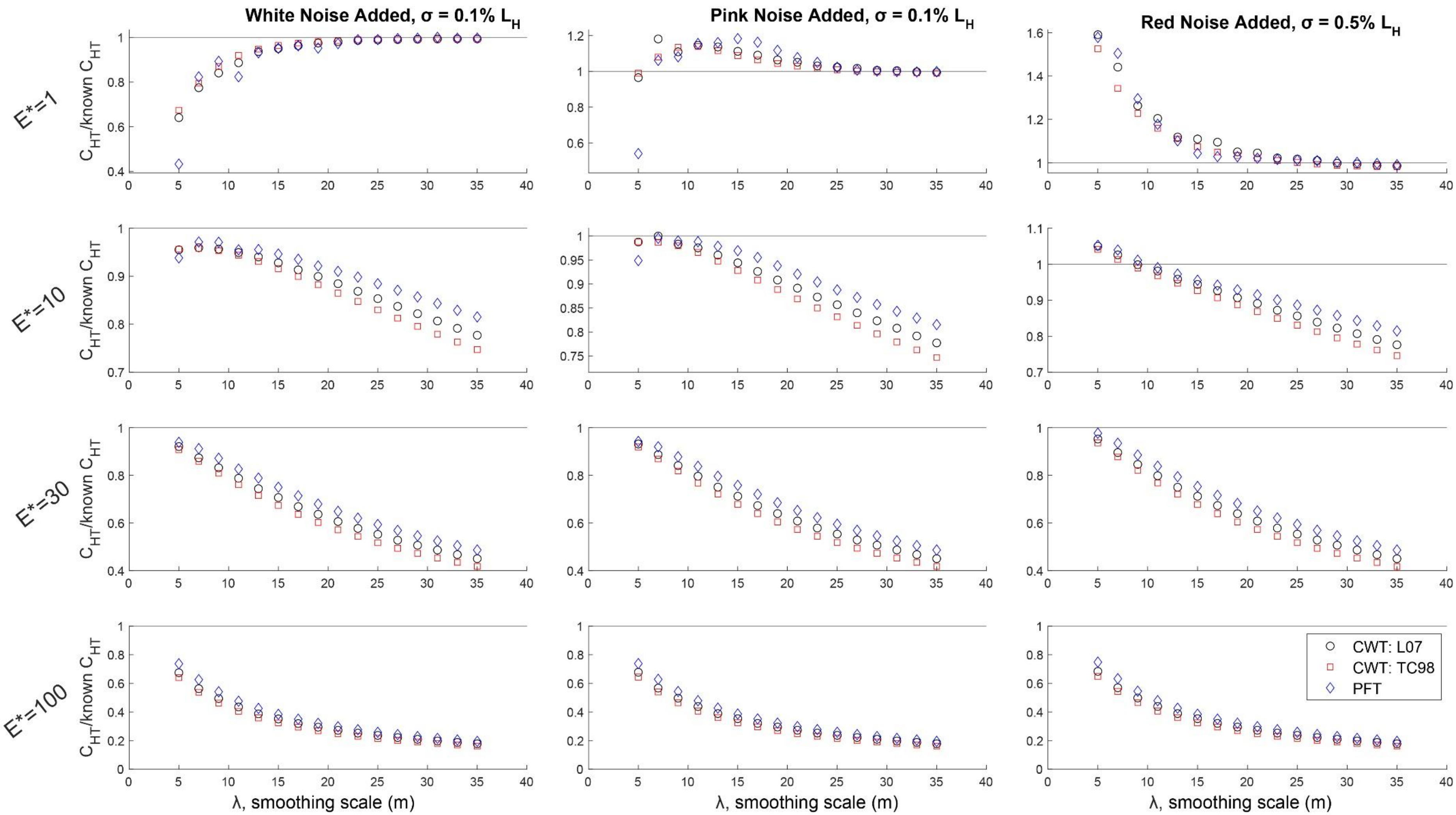

Figure S5: Ratio of C_{HT} of synthetic hillslopes where E*=1, 10, 30, and 100 measured at various smoothing scales, λ, with: σ=0.1% L_H white noise (first column), pink noise (second column), and red (Brownian) noise (third column). Ratio of C_{HT} is quantified as the quotient of the C_{HT} measured with the CWT or PFT and the actual synthetic C_{HT}. Black horizontal line in each panel corresponds with where the measured C_{HT} equals the actual synthetic C_{HT} (i.e. ratio=1). Points that plot above the line correspond with locations where C_{HT} is overestimated; points that plot below are underestimations. Note that compared to Figure 9 (σ=0.5%L_H), deviation between the measured and actual synthetic C_{HT} is less prominent at slow erosion rates (E*=1-10), though E* is still underestimated when E*=10. This is not unexpected given the underestimation of E* when no noise is added to the surface (see first column in Figure 9).

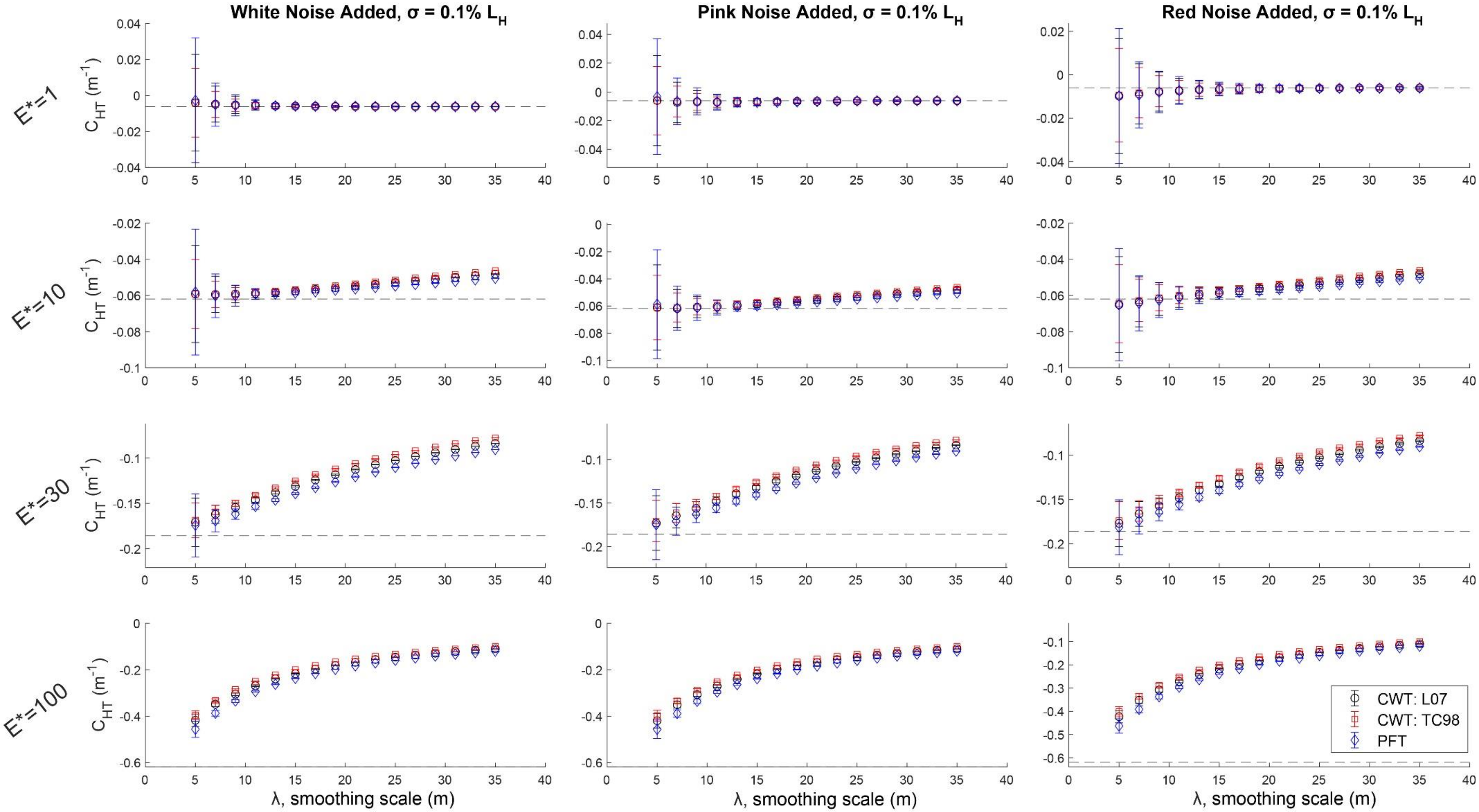

Figure S6: Hilltop curvature when noise amplitude σ=0.1% L_H. E* increases from E*=1 in top row to E*=100 in bottom row. Left column corresponds to synthetic hillslope is no added noise, while columns 2-4 correspond with hillslopes where white, pink, and red noise have been added, respectively. Error bars are 1σ standard deviation on the hilltop. Dashed black line is known C_{HT} from the synthetic hillslope. For clarity of deviation between measured and known C_{HT}, see the ratio of the two values in Figure S5.

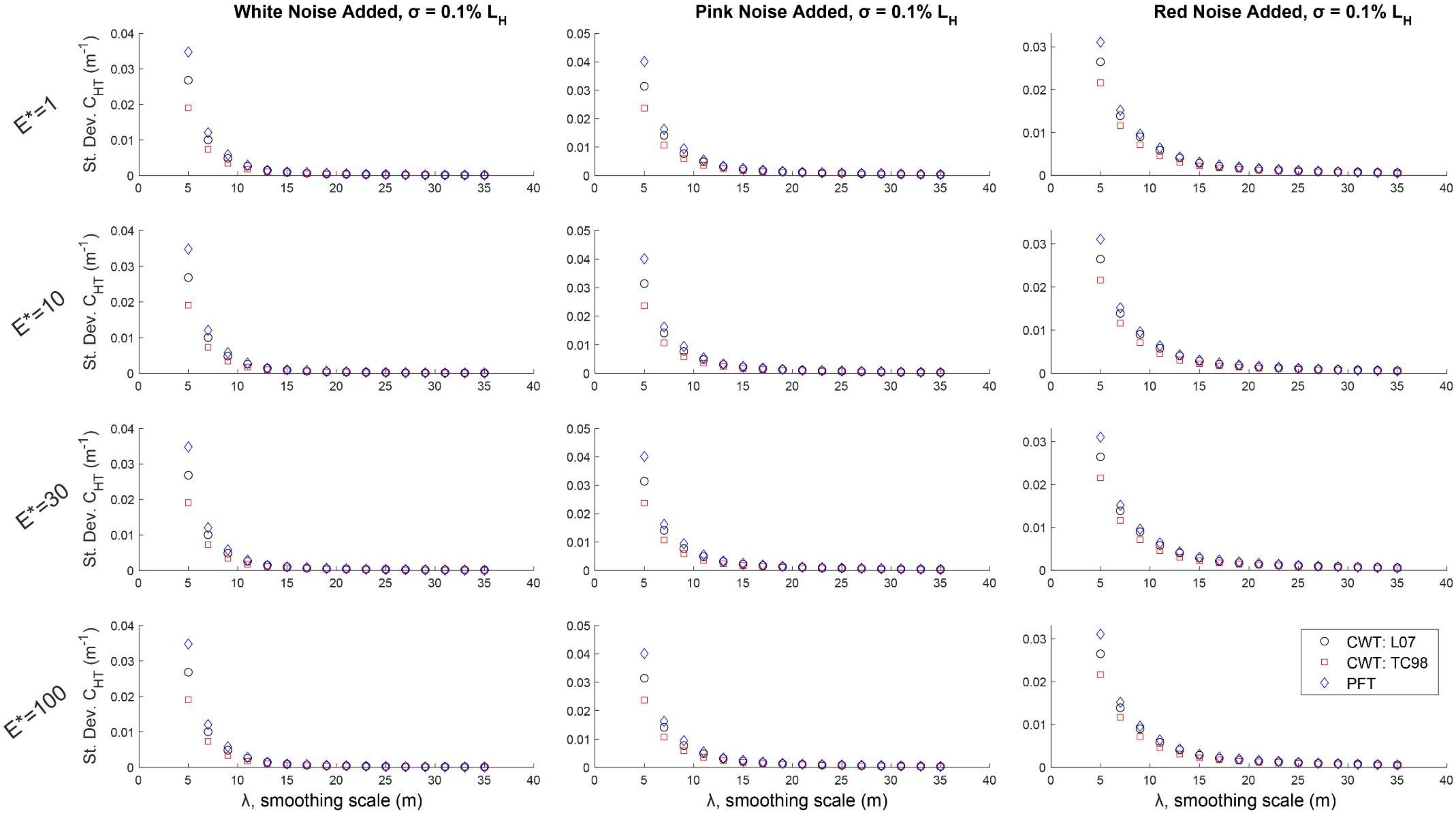

Figure S7: Standard deviation of C_{HT} for noise amplitude σ=0.1%L_H. These values correspond to the error bars in Figure S6. Note that surface noise does not vary as a function of E*. Therefore, given the distributive property of convolutions (see main text for details), the standard deviation does not vary with E*. Note that the standard deviation is high at small smoothing scales when the signal to noise ratio is high. As topography is smoothed, the uncertainty in C_{HT} along the hilltop decreases.

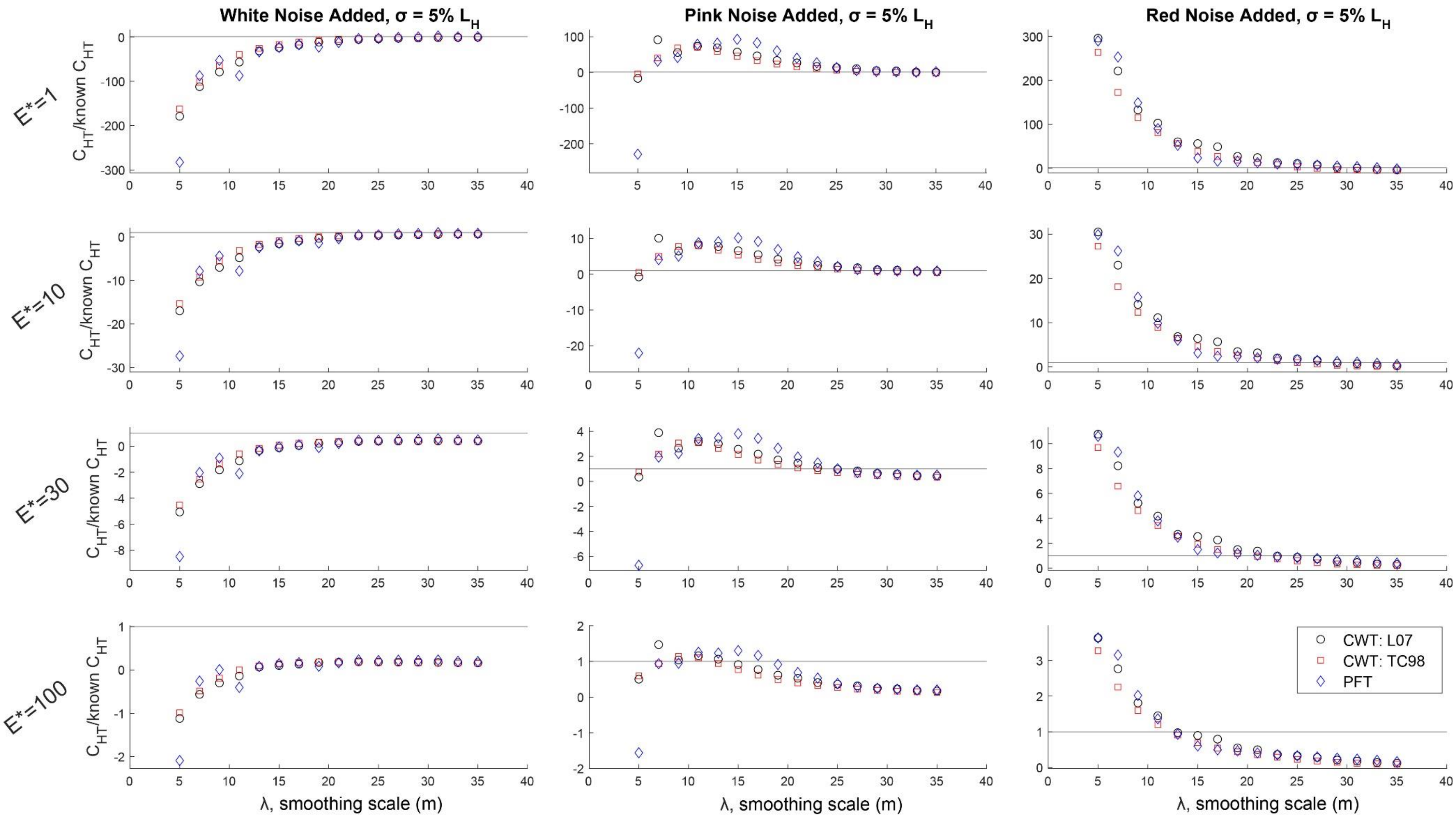

Figure S8: Ratio of C_{HT} for synthetic hillslopes where E*=1, 10, 30, and 100 measured at various smoothing scales, λ, with: σ=5% L_H white noise (first column), pink noise (second column), and red (Brownian) noise (third column). Ratio of C_{HT} is quantified as the quotient of the C_{HT} measured with the CWT or PFT and the actual synthetic C_{HT}. Black horizontal line in each panel corresponds with where the measured C_{HT} equals the actual synthetic C_{HT} (i.e. ratio=1). Points that plot above the line correspond with locations where C_{HT} is overestimated; points that plot below are underestimations. Note that compared to Figure 9 (σ=0.5%L_H), deviation between the measured and actual synthetic C_{HT} is prominent at all erosion rates. While measured C_{HT} does converge towards the actual value for E*=1-30, note the greatly extend y-axes. Furthermore, in real landscapes, positive valley curvatures will begin to be introduced at these scales. Noise amplitudes in excess of 5 m are likely unphysical in real landscapes. However, this case demonstrates that noise remains a hindrance for curvature measurement techniques as amplitude increases. Care should be taken, therefore, in selecting adequate smoothing scales and quantifying topographic surface roughness. We also emphasize that as topographic noise approaches longer wavelengths, there may be noisy regions with curvatures that mimic the hilltop curvature at that scales. This is likely rare, but would depend on the measurement scale and, in the synthetic case, the iteration of noise generation.

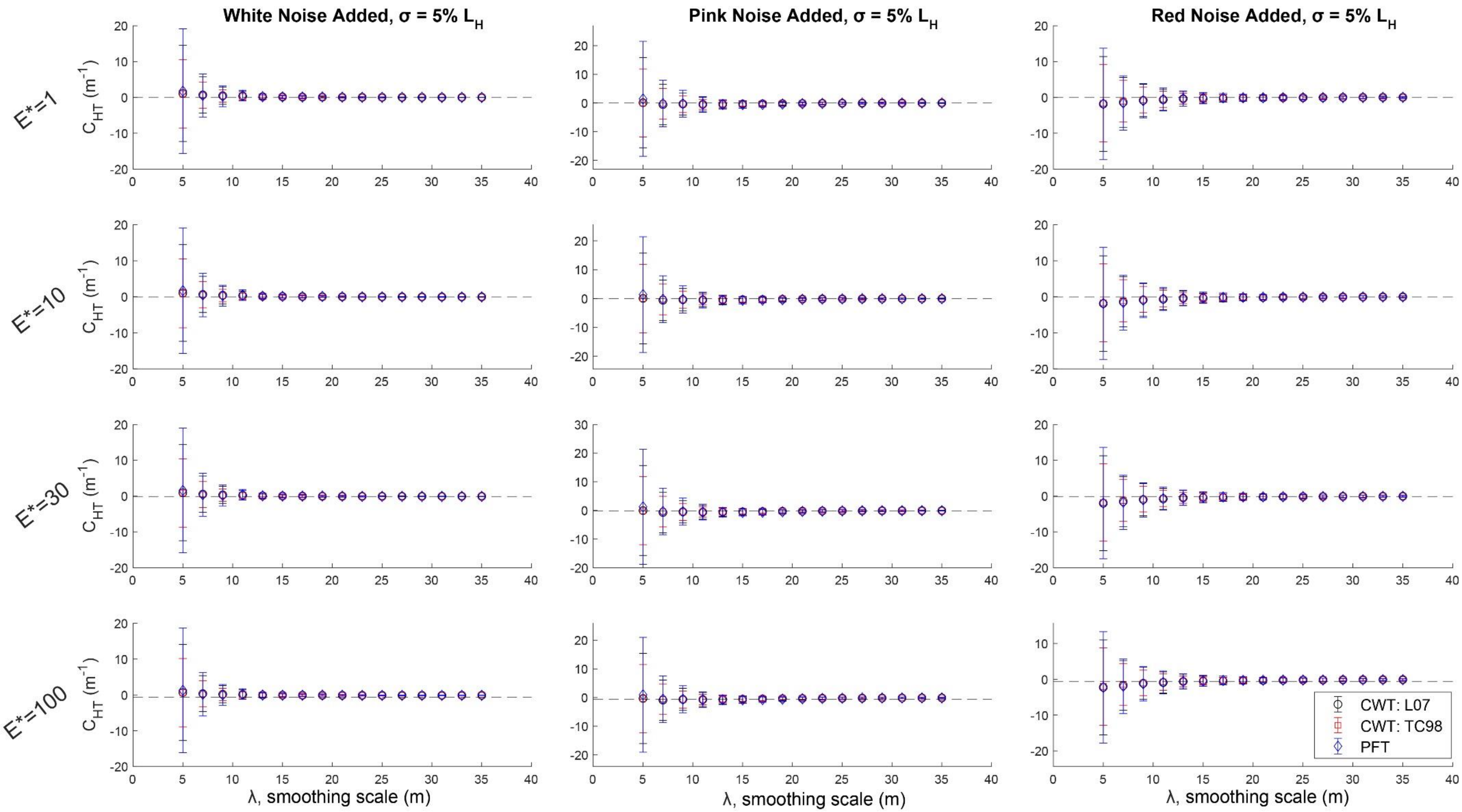

Figure S9: Hilltop curvature when noise amplitude σ=5% L_H. E* increases from E*=1 in top row to E*=100 in bottom row. Left column corresponds to synthetic hillslope is no added noise, while columns 2-4 correspond with hillslopes where white, pink, and red noise have been added, respectively. Error bars are 1σ standard deviation on the hilltop. Dashed black line is known C_{HT} from the synthetic hillslope. For clarity of deviation between measured and known C_{HT}, see the ratio of the two values in Figure S8.

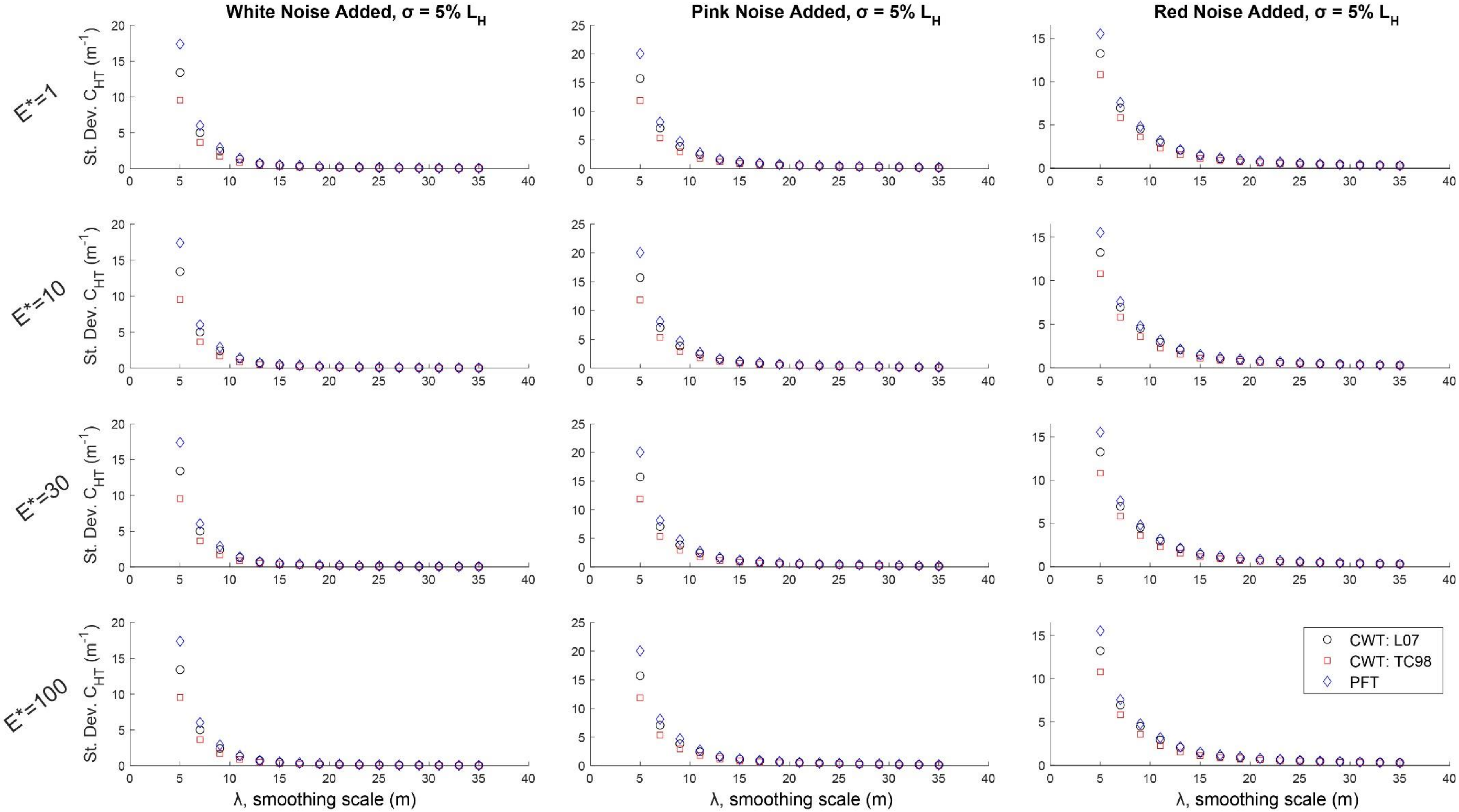

Figure S10: Standard deviation of C_{HT} for noise amplitude σ=5%L_H. These values correspond to the error bars in Figure S9. Note that surface noise does not vary as a function of E*. Therefore, given the distributive property of convolutions (see main text for details), the standard deviation does not vary with E*. Note that the standard deviation is high at small smoothing scales when the signal to noise ratio is high. As topography is smoothed, the uncertainty in C_{HT} along the hilltop decreases. Despite the high magnitude of the surface noise, the CWT and PFT still manage to output relatively consistent along-hilltop curvatures at larger smoothing scales.